Non-invasive liposome-mediated gene delivery can correct the ion transport defect in cystic fibrosis mutant mice

E.W.F.W. Alton, P.G. Middleton, N.J. Caplen, S.N. Smith, D.M. Steel, F.M. Munkonge, P.K. Jeffery, D.M. Geddes, S.L. Hart, R. Williamson, K.I. Fasold, A.D. Miller, P. Dickinson, B. J. Stevenson, G. McLachlan, J. R. Dorin & D. J. Porteous

Nature Genetics 5, 135–142 (1993)

The complete legend for Fig. 5 of this paper appears below.

Fig. 5 The mean responses of jejunum (*a* and *b*), ileum (*c* and *d*) and rectum (*e*) to forskolin (10 μM). Light shade, *cf/cf* (jejunum *n*=24, ileum *n*=7, rectum *n*=14); solid, treated (TR) (*n*=8 all tissues); dark, shade, +/+ (jejunum *n*=22, ileum *n*=9, rectum *n*=9). Error bars indicate SEM. All statistical comparisons refer to Isc measurements. +/+ v *cf/cf*: jejunum p<0.0001, ileum p=0.01, rectum p=0.0001; +/+ vs. TR: jejunum p<0.001, ileum p<0.05, rectum p<0.01; *cf/cf* vs. TR: jejunum p=0.78, ileum p=0.15, rectum p=0.24.

Tissue specific expression of *FMR-1* provides evidence for a functional role in fragile X syndrome

H. L. Hinds, C. T. Ashley, J. S. Sutcliffe, D. L. Nelson, S. T. Warren, D. E. Housman & M. Schalling

Nature Genetics 3, 36–43 (1993)

In this paper the legend to Fig. 2 was omitted. The following legend should have been published with Fig. 2.

Cloning of human, mouse and fission yeast recombination genes homologous to *RAD51* and *recA*

A. Shinohara, H. Ogawa, Y. Matsuda, N. Ushio, K. Ikea & T. Ogawa

Nature Genetics 4, 239–243 (1993)

In Fig. 1*a* of this paper, the amino acid sequence of *S. pombe* at positions 34 (A) and 274 (V) are incorrect and should be Q and L respectively (single letter amino acid code).

On the third page of this article (p. 241) the text in the first and second columns was transposed accidentally.

Introduction and expression of the 400 kilobase amyloid precursor protein gene in transgenic mice

B. T. Lamb, S. S. Sisodia, A. M. Lawler, H. H. Slunt, C. A. Kitt, W. G. Kearns, P. L. Pearson, D. L. Price & J. D. Gearhart

Nature Genetics 5, 22–30 (1993)

An unfortunate transposition rendered the title of this paper incorrect. The correct title is that printed above.

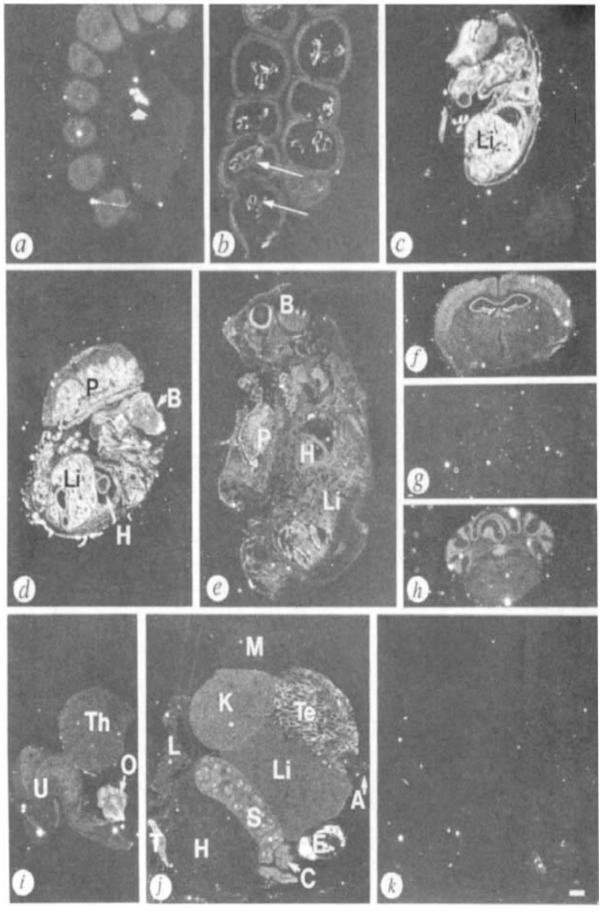

Fig. 2 *In situ* RNA hybridization with ^{35}S-labelled *fmr-1* oligonucleotide probe to sectioned murine whole embryos (*a–e*), brain (*f–h*) and peripheral organs (*j–k*). Film autoradiographs shown are after hybridization with the probes complementary to *fmr-1* mRNA (*a–i*) except for *g*, and the sense strand as a control probe (*g* and *k*) followed by 2 days (*a–b*), 10 days (*c–h*) or 2 wks (*j–k*) exposure (note differences in exposure times). *a*, Murine uterus at day 7 of pregnancy, labelling apparent throughout the uterine endometrium. Wide arrow indicates artefact/non-specific labelling. *b*, Multiple 10 day embryos shown within the maternal uterus, labelling still apparent in the uterine endometrium, though at slightly reduced levels. The embryos themselves (indicated in two of the uterine cavities by arrows) are uniformly labelled, with a particularly strong signal delineating the neural tube. *c*, 13 day embryo cut parasagittally. Strong hybridization is still evident, but at lower levels than at the 10 day embryonic stage and with a more heterogeneous expression pattern (Li, liver). *d*, 14 day embryo cut parasagittally with its accompanying placenta. Labelling is reduced compared to *c*, but remains widespread. Some individual organs such as the liver, gut and placenta are visible as regions of higher labelling (P, placenta; B, brain; Li, liver; H, heart). *e*, 19 day embryo cut parasagittally with its accompanying placenta (organs labelled as in *d*). Labelling is uniformly lower throughout the embryo with some individual organs such as the eye, brain, submandibular gland, thymus and placenta standing out as regions of higher labelling. *f*, Adult murine brain (coronal cross section). Intense labelling is apparent in the hippocampus and habenula, with diffuse labelling throughout the frontal lobe cortex and thalamus and a lack of labelling in the corpus callosum. *g*, Adjacent section to *f* hybridized with the sense probe FxS show random grain distribution. *h*, Adult murine cerebellum and brainstem (cross section). Intense labelling is apparent in the cerebellum with lower levels of labelling through the medulla. *i*, Multiple peripheral murine tissues (cross section). While expression is evident at uniformly low levels in the thyroid (Th) and uterus (U), very strong signals are visible in the ovary (O). *j*, Multiple peripheral murine tissues (cross section). Labelling seems to be absent in muscle (M), heart and aorta (A). Low levels of labelling are evident in the lung (L), with higher levels uniformly in the kidney (K), liver and colon (C). The testis (Te), spleen (S), thymus (T) and oesophagus (E) show distinct areas of strong hybridization. Multiple cross sections through the oesophagus are shown. *i*, Adjacent section to *h*, hybridized with the sense probe FxS showing random grain distribution. Scale bar, 1 mm in all autoradiographs.